International Journal of Chemical and Biochemical Sciences
(ISSN 2226-9614)

Journal Home page: www.iscientific.org/Journal.html

Effect of grinding techniques on *Chromolaena odorata* leaves for the biosynthesis of SnO_2 nanoparticles

[1]*Irmaizatussyehdany Buniyamin*, [1,3]*Rabiatuladawiyah Md Akhir*[3], [1,3]*Noor Asnida Asli*, [1,3]*Zuraida Khusaimi and* [1,2]*Mohamad Rusop Mahmood*

[1]*NANO-SciTech Laboratory, Centre for Functional Materials and Nanotechnology (CFMN), Institute of Science, Universiti Teknologi MARA (UiTM), 40450 Shah Alam, Selangor, Malaysia,* [2]*NANO-ElecTronic Centre, Engineering College, Universiti Teknologi MARA (UiTM), 40450 Shah Alam, Selangor, Malaysia and* [3]*Faculty of Applied Sciences, Universiti Teknologi MARA (UiTM), 40450 Shah Alam, Selangor, Malaysia*

Abstract

In this study, tin oxide nanoparticles (SnO_2 NPs) were synthesized via a green protocol using bioactive compounds from *Chromolaena odorata* leaves which stand as a reducing and capping agent. The leaves underwent two types of grinding techniques to investigate which technique would provide bioactive compounds in effective concentration to assist the biosynthesis process; ball-mill and electronic blender. The prepared SnO_2 NPs were characterized by fourier-transform infrared (FTIR), x-ray diffraction analysis (XRD), field emission scanning electron microscopy (FESEM), energy dispersive x-ray spectroscopy (EDX) and UV-visible diffuse reflectance spectroscopy (DRS). FTIR spectra evidenced the pertinent functional groups of SnO_2 NPs. From XRD analysis, both samples developed in tetragonal structure whereby ball-mill and electronic blender techniques gave average crystallite size of 7.85 and 11.60 nm respectively. Uniform distribution of agglomerated spherical shape of SnO_2 NPs was observed from the FESEM images and EDX analysis confirmed the presence of Sn and O elements. The reflectance percentage of SnO_2 NPs was found to be 48% with energy band value of 3.13 eV produced from ball-mill technique, while 37% reflectance and 3.39 eV from latter technique. Band gap values suggested this synthesized SnO_2 NPs using both techniques are practical candidates for optical function.

Keywords: Tin oxide nanoparticles, *Chromolaena odorata*, bioactive compound, biosynthesis, band gap

Full length article **Corresponding Author*, e-mail: syehdany@uitm.edu.my, nanouitm@gmail.com

1. Introduction

The outstanding performance of n-type semiconductors tin (iv) oxide nanoparticles (SnO_2 NPs), which possess an energy band gap of 3.6 eV is well known [1]. It has similar advantages to the other oxide semiconductors materials such as Al_2O_3, ZnO, CuO, TiO_2 that possess commercial simplicity in processing practice and are less toxic [2]. The functionalities of SnO_2 NPs can be found in lithium-ion batteries [3], solar cells [4], gas sensing [5], catalyst [6], etc. The advanced surface area of the designed nanomaterials provides high efficiency in facilitating the applications at an ideal level [7].

The preparation of SnO_2 NPs is known using various techniques such as hydrothermal [8], microwave heating [9], sol-gel [10], laser ablation [11], microemulsion [12], etc. However, these techniques use toxic chemicals, utilize high energy and temperature, and are very expensive, limiting the industrial applications of SnO_2 NPs. At this point, scientists designed the green synthetic method, which offers advantages whereby they use friendly protocol and are economical. Notably, this protocol involves the exploitation of the plant extract and has been of significant interest, especially in the biosynthesis field [13-15].

The green synthesis using plant extract towards SnO_2 NPs had been carried out using *Plectranthus amboinicus* [16], *Persia Americana* [17], *Pruni spinosae* flos [18], *Aspalathus linearis* [19], *Cleistanthus collinus* [20], *Ficus carica* [21], *Daphne mucronata* [22], *Brassica oleracea* L. var. botrytis [23], *Calotropis gigantean* [24] and *Ziziphus jujube* [25]. Reports stated these approaches possessed simplicity, where the source of plants was abundant. Other than that, it offered a mild reaction environment and water media instead of toxic solvents.

Chromolaena odorata (*C. odorata*) is a perennial shrub in Malaysia that is sometimes used for medicinal purposes. The secondary metabolites of bioactive compounds were found in the leaves segment of *C. odorata*, such as polyphenols, alkaloids, essential oils and flavonoids. These bioactive compounds can perform two tasks towards the SnO_2 NPs biosynthesis mechanism: reducing and capping actions [26-27]. A specific flavonoid compound identified as quercetin-type (Figure 1) is the ideal applicant to accomplish the actions. This is attributed to the availability of the two neighboring hydroxyl groups that bonded to the aromatic group, which facilitate the reduction process followed by the capping activity of the subjected metallic Sn^{4+} of the precursor salt [28].

Here in this report, we demonstrate the preparation of SnO_2 NPs *via* a green approach using leaves of *C. odorata*. The leaves underwent two types of grinding techniques; ball mill and conventional blender, denoted as A and B throughout this report. The grinding technique approach reduced particle size and changed the original surface structure, thus expanding their solvent extraction qualities [29]. Leaves grinding was required to break down the cell wall and cut its size, which simplified the following extraction process by having increments in terms of the surface area; thus the leaves' cells would easily be penetrated with solvent [30]. It was demonstrated that small particle size increased the extraction yield [31] and gave a slight increment for total flavonoid extraction [32-33]. Having this in hand, applying ball-mill (A) and conventional blender (B) would indicate which technique is more effective towards the grinding process for *C. odorata* leaves. The release ability effectiveness of the bioactive compounds towards the preparation of SnO_2 NPs can be determined. The properties of the produced SnO_2 NPs are studied based on their morphology, structure and optical properties. This was conducted by using fourier-transform infrared (FTIR), x-ray diffraction (XRD), field emission scanning electron microscopy (FESEM), energy dispersive x-ray analysis (EDX) and UV-Vis diffuse reflectance spectrometer.

2. Materials and methods

2.1. Materials

The precursor salt, namely tin (IV) chloride pentahydrate ($SnCl_4.\ 5H_2O$) was obtained from Sigma-Aldrich, *C. odorata* leaves were collected from Kuala Selangor area, Malaysia and throughout the experimental activity, milli-Q water was utilized.

2.2. Methodology

The leaves of *C. odorata* were dried and 20 g was taken to grind using a ball-mill machine and later the fine powder was boiled into 100 ml of water. The heating process was appropriately conducted at 60-70^oC for 30 minutes until the color of the solution turned to be dark green. The extract solution was cooled, filtrated and stored at 4^oC. The mixing of 220 mL of *C. odorata* aqueous solution into 80 mL of $SnCl_4.5H_2O$ was performed for 3 hours at ambient temperature. Later, the centrifugation process took place for 15 minutes to separate the gelatinous pellet with the supernatant liquid, in which the gelatinous product was subjected to water removal process for 2 hours at 80°C. The dark solid was mashed and later calcined at 700°C for 3 hours [34-35]. Similar approach was applied for preparation of SnO_2 NPs using conventional blender.

2.3. Phytochemical test of C. odorata leaves

The identification of main bioactive compounds in *C. odorata* leaves was carried out by using chemical tests that were reported by former methods.

2.3.1. Test for phenols

A dropwise of 5% $FeCl_3$ (ferric (III) chloride) was added up to 2 ml of *C. odorata* extract to provide a black solution as the mark of phenols [36].

2.3.2. Test for flavonoid

The addition of 10 % aqueous sodium hydroxide (2 ml) was carried out into 4 ml of the *C. odorata* extract, which later produced a yellow coloration. The mark of flavonoids presence was noted based on the transformation of yellowish to colorless solution on subsequent addition of dilute hydrochloric acid [37].

2.3.3. Test for terpenoids

A similar volume ratio of *C. odorata* extract and chloroform was mixed well. Then it was cooled in a water container and added dropwise with 3 ml of concentrated H_2SO_4. The solution was left over for about 30 minutes. The presence of terpenoids was noted as there was a reddish-brown coloration developed at the interface [38].

2.3.4. Test for alkaloids (Keller-Kiliani Test)

A mixture containing a solution of 4.0 ml glacial acetic acid, a drop of 2.0 % $FeCl_3$, 10 ml of *C. odorata* extract and 1 ml of concentrated H_2SO_4 was prepared by consecutive addition and shaken well. Later, a brown ring was developed in the middle of the layers that proved the alkaloids compound presented in the leaves extract [39].

3. Results and discussion

3.1. Plausible mechanism of SnO_2 NPs

Figure 2 shows the probable reaction mechanism that takes place to furnish SnO_2 NPs. The association of the precursor salt solution ($SnCl_4.\ 5H_2O$) occurs with *C. odorata* leaves extract, specifically quercetin-type flavonoid. Later, cations of Sn^{4+} from precursor salt disseminate in the solution and build a complex by bridging with the active sites of the hydroxyl group of quercetin. In this case, two aromatic rings provide four hydroxyl groups that are compatible with tetravalent Sn^{4+} cation. This bridging

network is said to be responsible for keeping the polyphenolic molecules as one and inhibit accumulation. The calcination process is subjected to this product and SnO_2 NPs produced as the outcome [40].

3.2. FTIR analysis

Figure 3 represents the FTIR spectra of SnO_2 NPs produced using extract solution prepared using ball-mill (A) and conventional blender (B) techniques. From the figure, all the absorption bands correspond to functional groups of SnO_2, and no other foreign peaks are observed. The absorption band between 1952 and 2069 cm^{-1} represents the O-H group derived from water adsorption, while the band within 1558-1755 cm^{-1} indicates the vibration of Sn-OH bonding. Moreover, SnO_2 vibration mode is displayed from the absorption band around 893-1104 cm^{-1}, and the Sn-O group is evidenced by the appearance of a peak at 542-754 cm^{-1} [41-42].

3.3. X-ray diffraction (XRD)

Figure 4 shows the index of the XRD pattern for the prepared SnO_2 NPs, whereby it is found to have good compatibility with earlier report [43-44]. The planes of (110), (101), (200), (211), (220), (002), (310), (112), (301), (202), (321) and (222) is associated to the appearance of the peaks at 2θ values of 26.9°, 34.1°, 38.2°, 51.5°, 54.4°, 57.6°, 61.6°, 64.4°, 65.6°, 70.9°, 78.4° and 83.3° respectively according to JCPDS card no. 01-077-0452. Based on the spectroscopic data, no foreign phases have been discovered and the construction of SnO_2 is recommended as a tetragonal structure [45]. Moreover, the sharpness pattern of the spectra indicates the crystallinity of the produced SnO_2 NPs. Furthermore, Full Width at Half Maximum (FWHM) is calculated based on the prominent plane (110) for crystallite size measurement using Scherrer's equation (1):

$$\mathbf{D = k\lambda/\beta\cos\theta \ldots \ldots \ldots (1)}$$

where k is the unknown shape factor, λ is the X-ray wavelength of Cu Kα (1.54 Å), β is the full width at the half maximum in radians and θ is the Bragg's angle. From the calculation, the average particle size for samples A and B is found to be 7.8 and 11.6 nm, respectively. It is observed that the synthesized SnO_2 NPs utilize extract, being ground by conventional blender furnishes a narrower and pronounced peak that indicates intensified crystallinity associated with better construction of SnO_2 NPs.

3.4. FESEM and EDX analysis

The morphology feature of biosynthesized SnO_2 NPs is displayed in FESEM images (Figure 5), which reveal an agglomerated spherical-like shape with diameter in nanoscale, uniform distribution, and crystalline nature. The produced SnO_2 NPs give measured diameters of 8.06 and 9.19 nm for samples A and B, respectively. According to EDX spectra, the primary peaks are observed at 0.5 and 3.5 eV corresponding to Sn and O elements, certifying constituents' existence [46]. Hence, it validates the construction of pure SnO_2 and gives 35 % of O weight percentages and 65 % Sn. In addition, at 0.1, 0.2 and 0.3 eV, some small peaks are also being noted that belong to chlorine (Cl), nitrogen (N) and carbon (C).

3.5. UV-visible diffuse reflectance analysis

The analysis result of the diffuse reflectance spectroscopy delivers valuable knowledge about the optical properties of the product [47]. Figure 6 demonstrates the optical transitions process represented by the strong decline at absorption edge at 500 nm in visible regions, with sample A resulting reflectance at 48 % while 37 % for sample B. The higher reflectance value for sample A presumably originated from smaller particles and larger surface volume, evidenced by the XRD and FESEM results. This reflectance result shows that utilizing *C. odorata* extract prepared from ball mill grinding would furnish SnO_2 NPs with better reflective capability than the latter technique.

The conversion of the reflectance values to absorbance was carried out based on Kubelka-Munk (KM) function (2) [48-49]. According to (2), at any appropriate wavelength as given in formula:

$$\mathbf{F(R)=(1-R)^2/2R=k/s \ldots \ldots \ldots (2)}$$

where F(R) is the Kubelka-Munk functions, and k, s are the K-M scattering and absorption coefficients. Figure 7 shows the linearity of the plotting and employment of the photon energy axis (x-axis) and by having this in hand, the acquisition of the band gap values can be accomplished. Samples A and B result in a band gap value of 3.13 and 3.39 eV respectively. Sample A having band gap value that is close to 3.10 eV which belongs to the structural band gap of the improved SnO_2 material [50]. However, both band gap values are still secured within the range of practice for application, especially for photocatalytic activity [51-53].

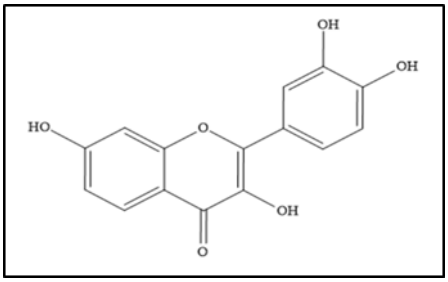

Fig. 1. Quercetin-type flavonoid

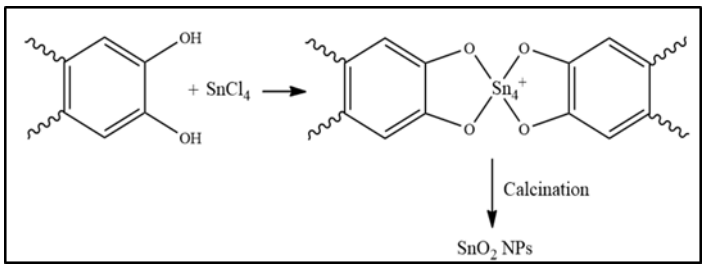

Fig. 2. Plausible mechanism for the construction of SnO_2 NPs

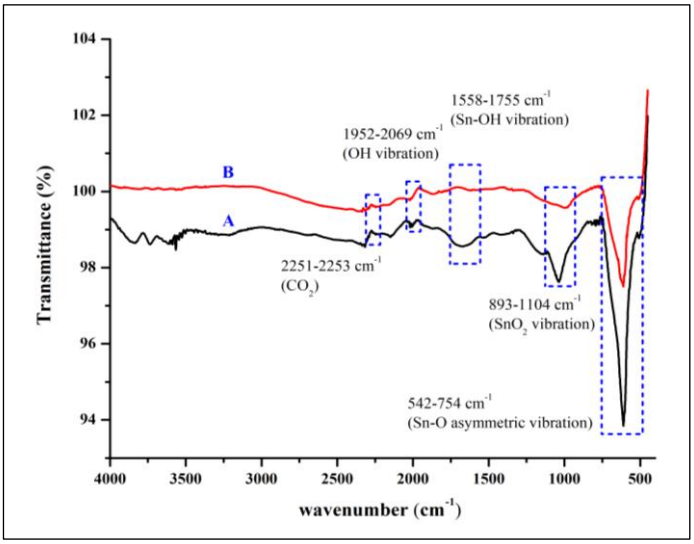

Fig. 3. FTIR spectra of SnO_2 NPs prepared using ball-mill (A) and conventional blender (B) techniques

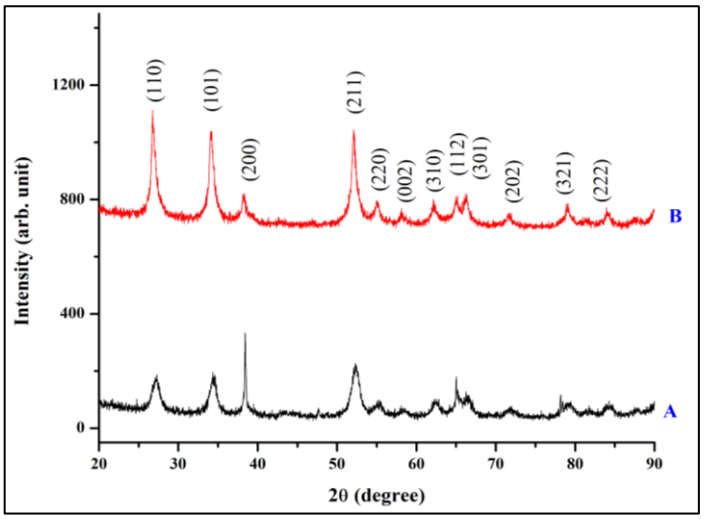

Fig. 4. XRD spectra of SnO_2 NPs using ball-mill (A) and conventional blender (B) techniques

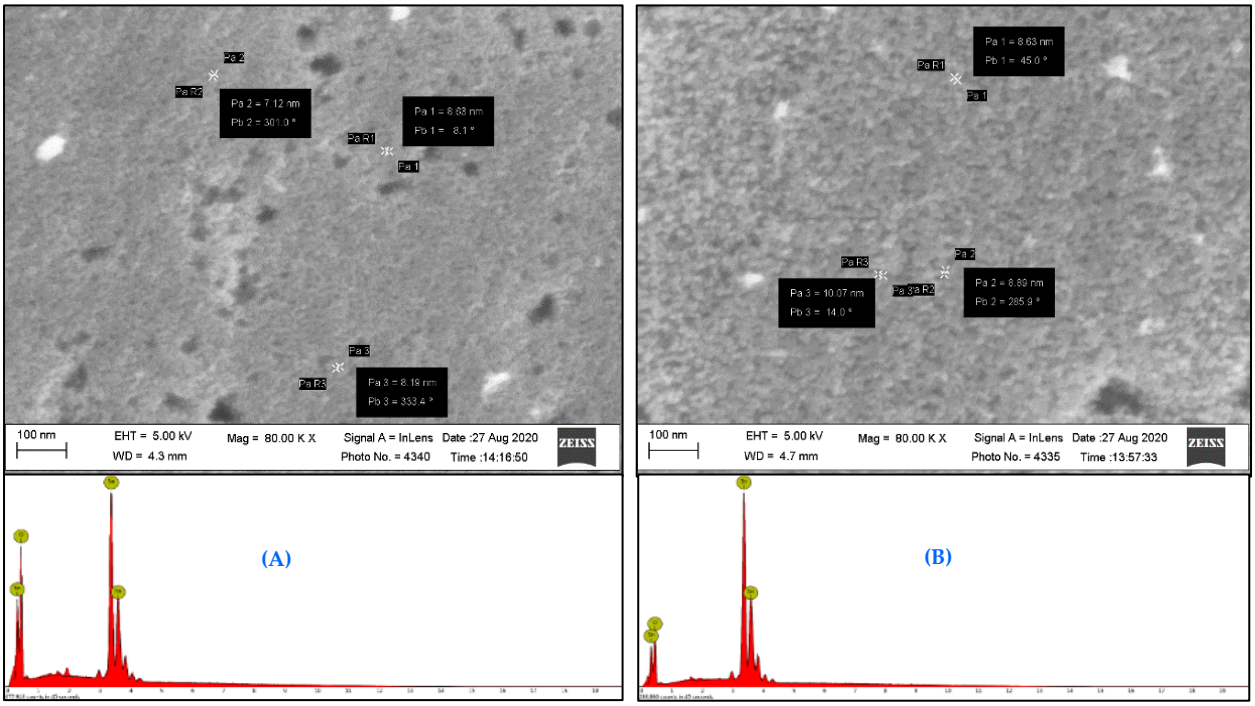

Fig. 5. FESEM and EDX images of SnO_2 NPs

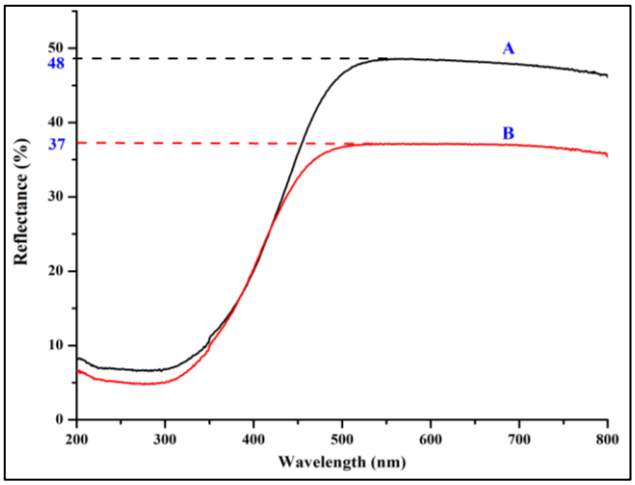

Fig. 6. UV-Vis diffuse reflectance spectra of SnO_2 NPs using ball-mill (A) and conventional blender (B) techniques

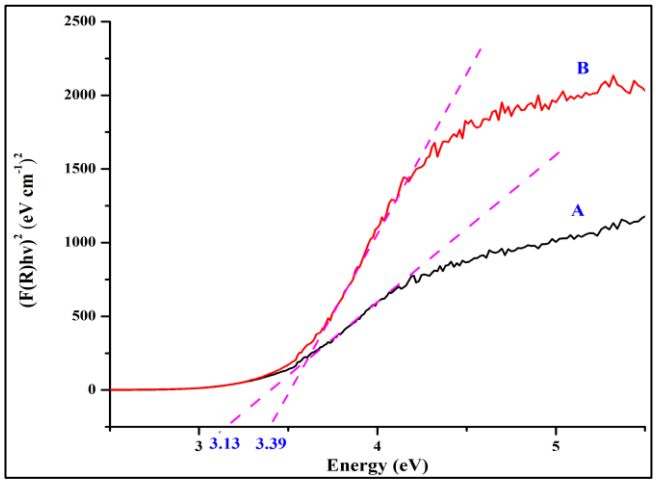

Fig. 7. (F(R) hv)^2 versus energy plots of SnO_2 NPs using ball-mill (A) and conventional blender (B) techniques

4. Conclusions

As for the conclusion, this study demonstrated that by applying a green protocol of biosynthesis, SnO_2 NPs had been effectively being produced using the exact solution of *C. odorata* leaves, in which the leaves underwent treatment of grinding; ball-mill and conventional blender. Both techniques proved to be effective in furnishing the bioactive compounds required for the biosynthesis process. From the result, FTIR obtained absorption bands correspond to the functional groups of SnO_2 construction. XRD resulted in an average crystallite size of 7.8 and 11.6 nm for SnO_2 NPs produced from the aforementioned technique shown and indicated as tetragonal structure. FESEM images showed SnO_2 NPs morphology of agglomerated spherical-like, uniform distribution and crystalline nature, whereby EDX analysis confirmed the presence for both elements. Based on diffuse reflectance analysis, the incident light was reduced at 48 % by using the first technique, resulting in a 3.13 eV band gap value, and 37 % reflectance for the latter technique with 3.39 eV. İt is found that the obtained band gap is not of much divergent value and still within the practical requirement for applications such as photocatalytic.

Acknowledgements

The author's acknowledge Institute of Science Universiti Teknologi MARA for their support in research by providing the facilities.

References

[1] A.N. Naje, A.S. Norry and A.M. Suhail. (2013). Preparation and characterization of SnO_2 nanoparticles. International Journal of Innovative Research in Science, Engineering and Technology (IJIRSET). 02: 7068-7062.

[2] S. Basu, A.C. Odena and I.F.J. Vankelecom. (2011). MOF-containing mixed-matrix membranes for CO_2/CH_4 and CO_2/N_2 binary gas mixture separations. Journal of Separation and Purification Techniques. 81: 31-40.

[3] F. Zoller, D. Böhm, T. Bein and F. Rohlfing. (2019). Tin oxide based nanomaterials and their application as anodes in lithium-ion batteries and beyond. ChemSusChem. 12: 4140-4159.

[4] S.N.F. Zainudin, H. Abdullah and M. Markom. (2019). Electrochemical studies of tin oxide based-dye-sensitized solar cells (DSSC): A Review. Journal of Materials Science: Materials in Electronics. 30: 5342-5356.

[5] Y. Wang, L. Liu, F. Sun, T. Li, T. Zhang and S. Qin. (2021). Humidity-insensitive NO_2 sensors based on SnO_2/rGO composites. Frontier Chemistry. 09: 681313.

[6] P. Manjunathan, V.S. Marakatti, P. Chandra, A.B. Kulal, S.B. Umbarkar, R. Ravishankar and G.V. Shanbhag. (2018). Mesoporous tin oxide: An efficient catalyst with versatile applications in acid and oxidation catalysis. Catalysis Today. 309: 61-76.

[7] J. Jeevanandam, A. Barhoum, Y.S. Chan, A. Dufresne and M.K. Danquah. (2018). Review on nanoparticles and nanostructured materials: history, sources, toxicity and regulations. Beilstein Journal of Nanotechnology. 09: 1050-1074.

[8] H.C. Chiu and C.S. Yeh. (2007). Hydrothermal synthesis of SnO_2 nanoparticles and their gas-sensing of alcohol. The Journal of Physical Chemistry C. 111: 7256-7259.

[9] A.K. Singh and U.T. Nakate. (2013). Microwave synthesis, characterization and photocatalytic properties of SnO_2 nanoparticles. Advances in Nanoparticles. 02: 66-70.

[10] M. Aziz, S. Saber Abbas and W.R. Wan Baharom. (2013). Size-controlled synthesis of SnO_2 nanoparticles by sol-gel method. Materials Letters. 91: 31-34.

[11] M.A. Gondal, Q.A. Drmosh and T.A. Salleh. (2010). Preparation and characterization of SnO_2 nanoparticles using high power pulsed laser. Applied Surface Science. 256: 7067-7070.

[12] N. Zamand, A.N. Pour, M.R. Housaindokht and M. Izadyar. (2014). Size-controlled synthesis of SnO_2 nanoparticles using reverse microemulsion method. Solid State Sciences. 33: 6-11.

[13] P.D. Shankar, S. Shobana, I. Karuppusamy, A. Pugazhendhi, V.S. Ramkumar, S. Arvindnarayan and G. Kumar. (2016). A review on the biosynthesis of metallic nanoparticles (gold and silver) using bio-components of microalgae: formation mechanism and applications. Enzyme and Microbial Technology. 95: 28-44.

[14] I. Buniyamin, R.M. Akhir, N.A. Asli, Z. Khusaimi and M. Rusop. (2021). Biosynthesis of SnO_2 nanoparticles by aqueous leaves extract of *Aquilaria malaccensis* (Agarwood), IOP Conference Series. Material Science and Engineering. 1092: 012070.

[15] R.M. Akhir, S.Z. Umbaidilah, N.A. Abdullah, I. Buniyamin, M. Rusop and Z. Khusaimi. (2021). Comparative study on morphology, structural and optical properties of non-seeded and seeded ZnO nanorods. In Recent Trends in Manufacturing and Materials Towards Industry. 961-969.

[16] L. Fu, Y. Zheng, Q. Ren, A. Wang and B. Deng. (2015). Green biosynthesis of SnO_2 nanoparticles by *Plectranthus amboinicus* Leaf extract their photocatalytic activity toward rhodamine B degradation. Journal of Ovonic Research. 11: 21-26.

[17] G. Elango and S. Mohana Roopan. (2016). Efficacy of SnO_2 nanoparticles toward photocatalytic

degradation of methylene blue dye. Journal of Photochemistry & Photobiology, B: Biology. 155: 34-38.

[18] R. Dobrucka, J. Dlugaszewska and M. Kaczmarek. (2019). Cytotoxic and antimicrobial effect of biosynthesized SnO_2 nanoparticles using *Pruni Spinosae* Flos Extract. Inorganic and Nano-Metal Chemistry. 01: 367-376.

[19] A. Diallo, E. Manikandan, V. Rajendran and M. Maaza. (2016). Physical and enhanced photocatalytic properties of green synthesized SnO_2 nanoparticles via *Aspalathus linearis*. Journal of Alloys and Compounds. 681: 561-570.

[20] P. Kamaraj, R. Vennila, M. Arthanareeswari and S. Devikala. (2014). Biological activities of tin oxide nanoparticles synthesized using plant extract. World Journal of Pharmacy and Pharmaceutical Sciences. 03: 382-388.

[21] J. Hu. (2015). Biosynthesis of SnO_2 nanoparticles by fig (*Ficus carica*) leaf extract for electrochemically determining Hg(II) in water samples. International Journal of Electrochemical Science. 10: 10668-10676.

[22] S. Haq, W. Rehman, M. Waseem, A. Shah, A.R. Khan, M.U. Rehman, P. Ahmad, B. Khan and G. Ali. (2020). Green synthesis and characterization of tin dioxide nanoparticles for photocatalytic and antimicrobial studies. Mater Research Express. 7: 025012.

[23] J. Osuntokun, D.C. Onwudiwe and E.E. Ebenso. (2017). Biosynthesis and photocatalytic properties of SnO_2 nanoparticles prepared using aqueous extract of cauliflower. Journal of Cluster Science. 1-14.

[24] T.T. Bhosale, H.M. Shinde, N.L. Gavade, S.B. Babar, V.V. Gawade, S.R. Sabale, R.J. Kamble, B.S. Shirke and K.M. Garadkar. (2018). Bio-synthesis of SnO_2 nanoparticles by aqueous leaf extract of *Calotropis gigantea* for photocatalytic applications. Journal of Materials Science: Materials in Electronics. 29: 1-10.

[25] M. Honarmand, M. Golmohammadi and A. Naeimi. (2019). Biosynthesis of tin oxide (SnO_2) nanoparticles using Jujube fruit for photocatalytic degradation of organic dyes. Advanced Powder Technology. 30: 1551-1557.

[26] A.G. Omokhua, L.J. Mcgaw, J.F. Finnie and J.V. Staden. (2016). *Chromolaena odorata* (L.) R.M. King & H. Rob. (Asteraceae) in Sub-Saharan Africa: A synthesis and review of its medicinal potential. Journal of Ethnopharmacology. 183: 112-122.

[27] A.C. Akinmoladun, E.O. Ibukun and I.A. Dan-Ologe. (2007). Phytochemical constituents and antioxidant properties of extracts from the leaves of *Chromolaena odorata*. Scientific Research and Essay. 02: 191-194.

[28] N. Panche, A.D. Diwan and S.R. Chandra. (2016). Flavonoids: An Overview. Journal of Nutrition Science. 05: 47.

[29] R.A.O. Thalita, D.O. Jacqueline, M.C.G. Eduardo, F.S. Marta Helena, G. Karina, F.D.S.V. Thais Maria and S. Erick. (2019). Benefits of superfine grinding method on antioxidant and antifungal characteristic of Brazilian green Propolis Extract. Scientia Agricola. 76: 398-404.

[30] N.S. Shiv, R. Sunil and K.T. Man. (2017). Antibacterial effects of Thuja leaves extract. International Journal of Applied Science and Biotechnology. 05: 256-260.

[31] O. Bensebiaa, D. Barthb, B. Bensebiaa and A. Dahmania. (2009). Supercritical CO_2 extraction of Rosemary: Effect of extraction parameters and modelling. Journal of Supercritical Fluids. 49: 161-166.

[32] J. Li, X. Qi-Xin, Q. Mu, M. Fei-Fei, T. Kiran and W. Zhao-Jun. (2017). Effect of superfine grinding on properties of *Vaccinium bracteatum* Thunb leaves powder. Food Science and Biotechnology. 1-8.

[33] Z. Ali, B. Loïc, K. Marie-Céleste and D. Amadou. (2016). Effect of particle size on antioxidant activity and catechin content of green tea powders. Journal of Food Science and Technology. 1-8.

[34] I. Buniyamin, R.M. Akhir, N.A. Asli, Z. Khusaimi and M. Rusop. (2021). Effect of calcination time on biosynthesised SnO_2 nanoparticles using bioactive compound from leaves extract of *Chromolaena odorata*. AIP Conference Proceedings. 2368: 020006.

[35] I. Buniyamin, R.M. Akhir, N.A. Asli, Z. Khusaimi and M. Rusop. (2021). Green synthesis of tin oxide nanoparticles by using leaves extract of *Chromolaena odorata*: The effect of different thermal calcination temperature to the energy band gap. Materials today: Proceedings. 48: 1805-1809.

[36] H. Usman, F.I. Abdulrahman and A. Usman. (2009). Qualitative phytochemical screening and in vitro antimicrobial effects of methanol stem bark extract of *Ficus thonningii* (Moraceae). African Journal of Traditional, Complementary and Alternative Medicines. 06: 275-280.

[37] R. Dhivya and K. Manimegalai. (2013). Preliminary phytochemical screening and GC-MS profiling of ethanolic flower extract of *Calotropis Gigantea* Linn. (Apocynaceae). Journal of Pharmacognosy and Phytochemistry. 02: 28-32.

[38] V.N. Verma. (2013). The chemical study of Calotropis. International Letters of Chemistry, Physics and Astronomy. 20: 74-90.

[39] R. Gul, S.U. Jan, S. Faridullah, S. Sherani and N. Jahan. (2017). Preliminary phytochemical screening, quantitative analysis of alkaloids, and antioxidant activity of crude plant extracts from *Ephedra intermedia* indigenous to Balochistan. The Scientific World Journal. 5873648.

[40] V.V. Gawade, N.L. Gavade, H.M. Shinde, S.B. Babar, A.N. Kadam and K.M. Garadkar. (2017). Green synthesis of ZnO nanoparticles by using *Calotropis procera* leaves for the photodegradation of methyl orange. Journal of Materials Science: Materials in Electronics. 28: 14033-14039.

[41] R. Rahmi and F. Kurniawan. (2017). Synthesis of SnO_2 nanoparticles by high potential electrolysis. Bulletin of Chemical Reaction Engineering & Catalysis. 12: 281-286.

[42] A.R. Razeghizadeh, L. Zalaghi, I. Kazeminezhad and V. Rafee. (2017). Growth and optical properties investigation of pure and Al-doped SnO_2 nanostructures by sol-gel method. Iranian Journal of Chemistry and Chemical Engineering. 36: 1-9.

[43] V.K. Vidhu and D. Philip. (2015). Biogenic synthesis of SnO_2 nanoparticles: Evaluation of antibacterial and antioxidant activities. Spectrochimica Acta Part A: Molecular and Biomolecular Spectroscopy. 134: 372-379.

[44] G. Elango, S.M. Kumaran, S.S. Kumar, S. Muthuraja and S.M. Roopan. (2015). Green synthesis of SnO_2 nanoparticles and its photocatalytic activity of phenol sulfonphthalein Dye. Spectrochimica Acta part A – Molecular and Biomolecular Spectroscopy. 145: 176-180.

[45] S. Sudhaparimala, A. Gnanamani and A.B. Mandal. (2014). Green synthesis of tin based nano medicine: Assessment of microstructure and surface property. American Journal of Nanoscience and Nanotechnology. 02: 75-83.

[46] G.B. Hong and C.J. Jiang. (2017). Synthesis of SnO_2 nanoparticles using extracts from *Litsea cubeba* Fruits. Materials Letters. 194: 164-167.

[47] S.A. Saleh, A.A. Ibrahim and S.H. Mohamed. (2016). Structural and optical properties of nanostructured Fe-doped SnO_2. Acta Physica Polonica A. 129: 1220-1225.

[48] V. Senthilkumar, S. Karuppanan and P. Vickraman. (2012). Microstructural, electrical and optical properties of indium tin oxide (ITO) nanoparticles synthesized by co-precipitation method. Materials Research Bulletin. 47: 1051-1056.

[49] A. Ayeshamariam, S. Ramalingam, M. Bououdina and M. Jayachandranm. (2014). Preparation and characterizations of SnO_2 nanopowder and spectroscopic (FT-IR, FT-Raman, UV-Visible and NMR) analysis using HF and DFT calculations. Spectrochimica Acta part A: Molecular and Biomolecular Spectroscopy. 118: 1135-1143.

[50] A.M. Ganose and D.O. Scanlon. (2016). Band gap and work function tailoring of SnO_2 for improved transparent conducting ability in photovoltaics. Material Chemistry. C. 4: 1467-1475.

[51] J. Wang, C. Lu, X. Liu, Y. Wang, Z. Zhu and D. Meng. (2017). Synthesis of tin oxide (SnO & SnO_2) micro/nanostructures with novel distribution characteristic and superior photocatalytic performance. Materials and Design. 115: 103-111.

[52] E. Haritha, S.M. Roopan, G. Madhavi, G. Elango, N.A. Al-Dhabi and M.V. Arasu. (2016). Green chemical approach towards the synthesis of SnO_2 NPs in argument with photocatalytic degradation of diazo dye and its kinetic studies. Journal of Photochemistry & Photobiology, B: Biology. 162: 441-447.

[53] K. Prakash, P. Senthil Kumar, S. Pandiaraj, K. Saravanakumar and S. Karuthapandian. (2016). Controllable synthesis of SnO_2 photocatalyst with superior photocatalytic activity for the degradation of methylene blue dye solution. Journal of Experimental Nanoscience. 11: 1138-1155.